Eco-friendly recovery of pure and long carbon fibres from aged epoxy matrix composites by H2O2 as an oxidant

Mabalane P. N., Molnár K., Khalifa Y., Puskas J. E., Molnár K., Khoathane C.

Accepted for publication in JOURNAL OF MATERIAL CYCLES AND WASTE MANAGEMENT
Published in 2024
DOI: 10.1007/s10163-024-02126-y

Journal of Material Cycles and Waste Management (2025) 27:429–445
https://doi.org/10.1007/s10163-024-02126-y

ORIGINAL ARTICLE

Eco-friendly recovery of pure and long carbon fibres from aged epoxy matrix composites by H_2O_2 as an oxidant

Paul Njeni Mabalane[1] · Kristof Molnar[2,3] · Yehia Khalifa[4] · Judit E. Puskas[2] · Kolos Molnár[1,5,6,7] · Caroline Khoathane[1]

Received: 6 February 2024 / Accepted: 19 November 2024 / Published online: 4 December 2024

Abstract

In this study, we focused on the chemical recovery of carbon fibres from epoxy matrix composite wastes. First, we laminated and cured composite panels from carbon fibre-reinforced prepregs (CFRP) and then aged them under controlled circumstances to simulate their lifespan. Fibre recovery was then carried out by hydrogen peroxide (H_2O_2) at 6 bar and between 60 and 150 °C. We chose this material because it results in a rapid, cost-efficient, and environmentally friendly process. Besides, we expected it would allow the removal of the polymer matrix without fragmenting the fibres. We aimed to investigate the matrix decomposition in H_2O_2, the purity of the obtained fibres and the retention of their mechanical properties. The purity and the structure of the obtained carbon fibres were then characterised by using scanning electronic microscopy (SEM), X-ray diffraction (XRD), thermogravimetry (TGA), infrared spectroscopy (IR), and X-ray photoelectron spectroscopy (XPS). We found that H_2O_2 was effective in recovering carbon fibres, especially at 150 °C. The mechanical results showed that the retention of the modulus was complete, while the tensile strength and elongation at break decreased by 35% due to micro-structural damages. The fibres still have better properties than glass or basalt fibres; therefore, good-quality composites can be made using them.

✉ Kolos Molnár
molnar@pt.bme.hu

1 Department of Chemical, Metallurgical and Materials Engineering, Tshwane University of Technology, Pretoria, South Africa

2 Department of Food, Agricultural and Biological Engineering, Ohio Agricultural Research and Development Center, CFAES Wooster Campus, The Ohio State University, 1680 Madison Avenue, Wooster, OH 44691, USA

3 Laboratory of Nanochemistry, Department of Biophysics and Radiation Biology, Semmelweis University, Nagyvárad tér 4., Budapest 1089, Hungary

4 Department of Chemistry and Biochemistry, The Ohio State University, 100 West 18th Avenue, Columbus, OH 43210, USA

5 Department of Polymer Engineering, Faculty of Mechanical Engineering, Budapest University of Technology and Economics, Műegyetem rkp. 3, Budapest 1111, Hungary

6 HUN–REN–BME Research Group for Composite Science and Technology, Műegyetem rkp. 3., Budapest 1111, Hungary

7 MTA-BME Lendület Sustainable Polymers Research Group, Műegyetem rkp. 3, Budapest 1111, Hungary

Graphical Abstract

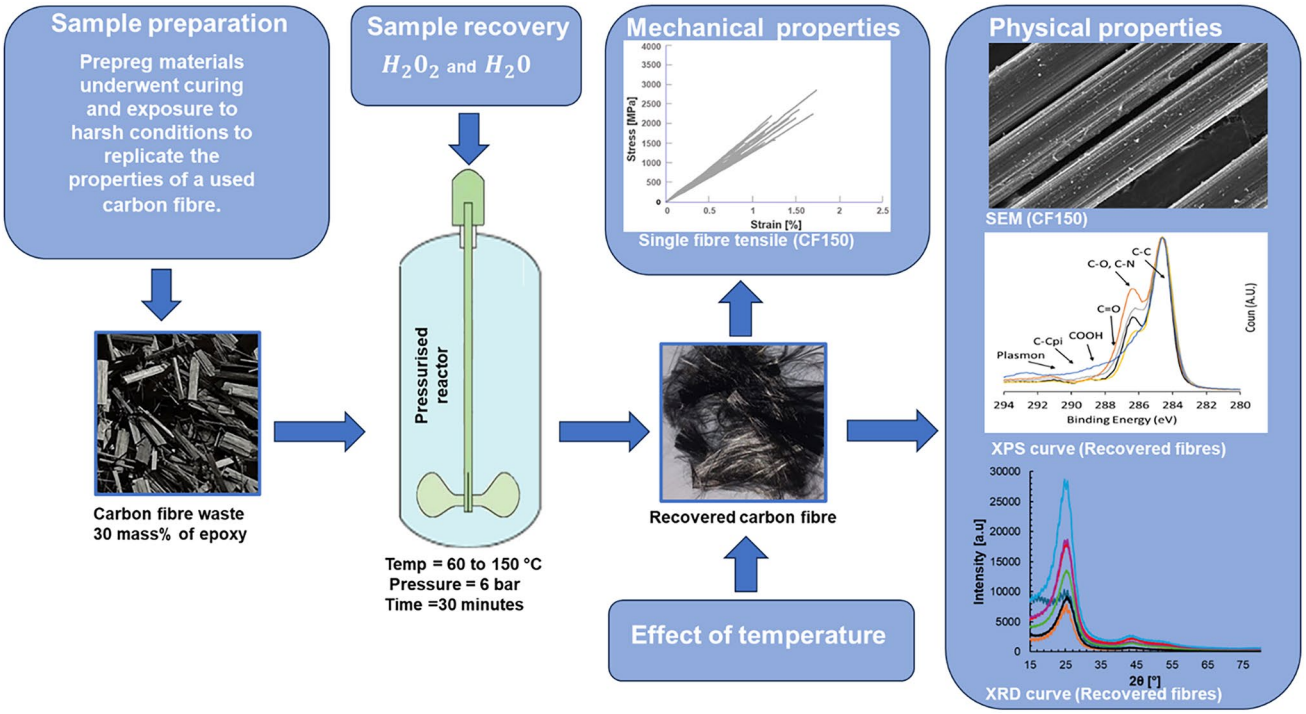

Keywords Carbon fibres · Chemical recovery · Mechanical properties · Environmental impact · Epoxy matrix degradation

Introduction

Carbon fibre-reinforced polymers (CFRPs) are widely used in various industries due to their excellent mechanical properties and lightweight nature. Reduced material weight in automobiles and aeroplanes also contributes to fuel economy and significantly reduces carbon dioxide (CO_2) emissions to the atmosphere [1, 2]. Besides the low density of CFRPs, they have excellent mechanical and thermal properties [3, 4]. CFRP is lightweight and possesses flexural strength and stiffness characteristics, impact resistance and fatigue behaviour [5]. Production methods for virgin carbon fibres (neat CF) must be economically viable. Besides that, one must consider the whole life cycle of these fibre and composite products. Most CFRP products go to landfills when their life span is reached, and landfilling poses an environmental concern and remains a global issue today [6, 7]. Thus, not just the production but also the disposal of CFRPs pose significant ecological challenges [8, 9]. To address these concerns, researchers have explored using recycled carbon fibres (rCF) in CFRPs as an eco-friendly alternative to neat CF.

Recycled fibres are recovered from production lines or from carbon composite materials that have reached their lifespan [10]. New, rapid, efficient, and eco-friendly technologies for recycling carbon fibres are required to reduce waste and environmental impact while maintaining their superior properties [10, 11].

Mechanical recycling entails grinding or shredding the composite materials to recover the carbon fibres [7, 10]. It is far from ideal since only short, fragmented fibres with a high residual matrix content can be obtained with deteriorated fibre properties compared to virgin fibres [12, 13].

Thermal methods like pyrolysis involve heating composite materials in a reduced oxygen environment. This controlled process decomposes the polymer matrix, allowing the separation of carbon fibres [14]. While this yields fibres and valuable by-products like pyrolysis gas and oil, the method has drawbacks [15]. The high temperatures required for pyrolysis lead to cost implications due to energy consumption and may compromise fibre quality [13, 16].

Carbon fibres are extracted from the matrix in a reducing or oxidising solution in chemical recycling processes [17]. Since carbon fibres are mainly used in thermoset matrices, which are robust, crosslinked structures, it is very challenging to gain high-purity fibres this way [10, 18, 19].

The thermoset and epoxy resin industries are highly regulated, particularly for applications in aerospace, automotive, and electronics. Regulations limit the use of hazardous materials, including heavy metals and certain flame retardants, to ensure safety and environmental compliance.

At current chemical recycling methods, unpleasant solvents such as subcritical acetone and supercritical methanol are used and can take a long time to decompose [10, 20]. However, there are eco-friendly approaches to sustainable development. For example, subcritical water can be used as an oxidation medium to decompose the epoxy resin; however, it requires a long reaction time, high pressure, high temperature and energy [20].

Another option is hydrogen peroxide (H_2O_2). It can be used in industry, requiring low temperatures and pressures compared to subcritical and near-subcritical water processes. During the decomposition mechanism of this approach, the hydroxyl groups (-OH) from hydrogen peroxide react with the amine group, forming a hydroperoxide intermediate at the nitrogen atom, leading to a nitrogen-oxide intermediate. Water is released during this process [21]. Depending on the processing temperature (60–150 °C), which this study investigates, heat accelerates nitrogen-oxide breakdown, cleaving the epoxy polymer and releasing imine (R_1–CH = NR_2) and other byproducts as highlighted in Fig. 1 [22, 23].:

As the temperature increases, molecules of H_2O_2 tend to have high kinetic energy that results in the formation of oxygen molecules, which help the oxidation or the decomposition of the polymer matrix [24].

There are reports on successful decomposition achieved through a mixture of H_2O_2 and acetone [23]. However, it is essential to note that acetone is a chemically spontaneous reagent with high expansion rates due to its high volatility. This characteristic of acetone poses a challenge to a smooth and well-controlled recovery process, particularly at moderate to high pressures.

Prolonged exposure to UV radiation can also cause the epoxy to degrade, resulting in a deterioration of mechanical properties, such as reduced strength, stiffness, and toughness [25]. The epoxy may also become brittle and prone to cracking or delamination. UV radiation can weaken this interface, leading to a loss of adhesion between the fibres and the epoxy [26]. It can lead to the breakdown of the epoxy resin at the surface, resulting in the formation of microcracks, crazing, or yellowing [27]. Current recycling methods for CFRPs have limitations regarding efficiency, cost, and the preservation of fibre properties.

Existing mechanical recycling technologies produce shredded carbon fibres, resulting in fibres being disintegrated, whilst thermal methods require an enormous amount of energy and high temperatures. Both methods mentioned above also contribute to the degradation of carbon fibre characteristics. As a result, it is critical to investigate measures to reduce these challenges. Innovative strategies for extracting carbon fibres more efficiently and cost-effectively are required.

The primary purpose of this research article was to develop recycling technologies that protect the mechanical and thermal properties of carbon fibres. This was accomplished using H_2O_2 as a solvent in a pressurised reactor. We prepared and cured carbon fibre-reinforced epoxy laminates, aged those to simulate their lifespan, and then recovered the carbon fibres from this simulated composite waste at various temperatures. We aimed to investigate the effect of ageing and recovery temperature on the purity, structure, and mechanical properties of carbon fibres.

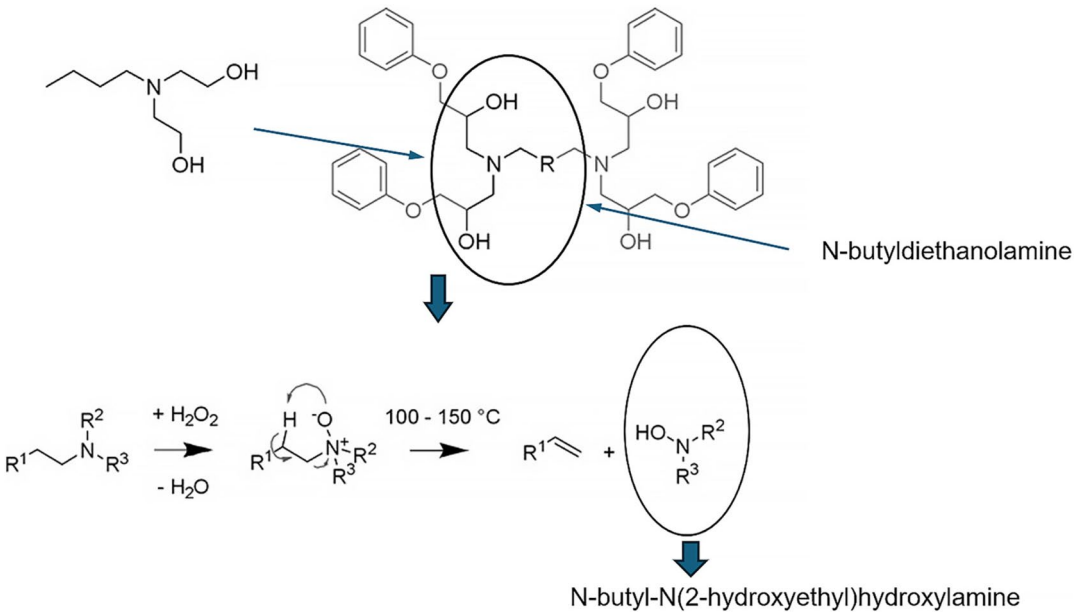

Fig. 1 Mechanism of epoxy resin decomposition adapted from ref. [21]

Experimental

Materials

Epoxy matrix pre-preg, type (CM-Preg F-P24 385/1250) with a 70 mass% nominal carbon fibre content (385 g/m^2 carbon fibre in 550 g/m^2 pre-preg) from c-m-p Gmbh. (Heinsberg, Germany) was used to prepare composite panels. The laminates were later aged, and the carbon fibres were recovered. Release film from AMT Composites (Cape Town, South Africa) was used to prevent bonding between the steel plate mould and the epoxy resin. We used a vacuum bag from the same company. The cured specimens were aged in a UV chamber, and then hydrogen peroxide (90%) from Sigma Aldrich (Massachusetts, USA) was used as an oxidising agent to decompose the matrix.

Preparation and curing of CFRP

The carbon fibre-reinforced pre-preg was cut into 20 × 50 mm pieces and placed into a flat mould covered with the release agent. We used two flat iron plates 300 × 150 mm moulds to shape the laminates to the specified dimension. The layers of pre-pregs were first hand-laid up within the mould. The fibres were placed in three layers with the same orientation. The mould was then closed and placed inside a vacuum bag. We used a vacuum pump (Speedivac, Cape Town, South Africa) to achieve negative pressure for compacting our laminates.

A high-pressure cyclotherm autoclave (300 L, Germiston, South Africa) was used to cure the laminates. The autoclave was used as per the ISO13000:2011 standard, and the venting mechanism was in place to keep the pressure gauge at zero bar. The samples were heated from room temperature to 126 °C at a ramp rate of 5 °C/min and held there for 2 h. This gradual temperature increase helped to ensure proper resin flow, minimise the risk of voids and defects, and promote uniform curing throughout the composite. Once the set conditions were reached and the 2 h elapsed, the mould was then allowed to cool before opening the chamber and then the mould.

Accelerated weathering of cured CFRP

We carried out the artificial weathering of the samples to simulate the long-term application of the composite panels (mimicked damage brought on by sunlight, rain, and dew). The prepared carbon fibre composite specimens were subjected to UV radiation and water vapour condensation using an accelerated weathering tester (QUV, QLAB, Saarbrucken, Germany). The QUV accelerated weathering chamber was set at the wavelength of 295–365 nm band and a temperature of 60 °C; the irradiance level was set to be 0.68 W/m^2 at 340 nm. The specimens (8 samples) were exposed to water vapour condensation at 60 °C and 100% humidity to achieve the harsh weather conditions. The specimens were exposed to weathering for 1000 h.

Carbon fibre recovery

We aimed to recover the carbon fibres from the weathered specimens to simulate the actual lifespan of the composites. The oxidation recovery process of carbon fibres was conducted in a 1-L Buchi reactor (Midiclave cc 07, Büchiglasuster, Switzerland). This stainless-steel high-pressure reactor was equipped with a rapture disc set at 40 bar, and it had a temperature range of − 20 °C to 300 °C. Hydrogen peroxide was employed as the oxidising agent to decompose the resin that is reinforced with the fibres.

For the oxidation process, a 200 mL mixture of hydrogen peroxide and water in a 1:1 ratio was carefully measured and poured into the reactor, which already contained 8 pieces of weathered specimens of CFRP short laminates (20 × 50 mm). To avoid any damage to the laminates and fibres, the stirrer was turned off during the process. A constant pressure of 6 bars was maintained using the control valve, and the desired constant temperature was achieved by utilising the water jacket of the reactor. The oxidation procedure was conducted for a duration of 30 min at single temperature points, between 60 °C and 150 °C with 10 °C increments. The temperature was constant throughout the experiment, but between 120 to 140 °C it was difficult to maintain steady conditions.

Following each 30-min interval at a designated constant temperature mentioned above, the reactor was allowed to cool down to room temperature. Subsequently, the resulting recycled products were carefully collected and labelled to cool down to room temperature naturally CF60 to CF150, where the number stands for the set temperature.

Following the oxidation, the recovered carbon fibres were subjected to a thorough washing process using acetone to remove any loosely connected impurities present on their surfaces.

Characterisation of the recovered carbon fibres

We measured the mass of the samples before and after ageing and after the recovery by H_2O_2.

The main purpose of mass measurement was to find the initial parameters; thus, we had only one sample per test, and there were no deviations calculated. Since we did not know the exact fibre content, the fibre contents were only estimates. On the other hand, it helped us to find the most characteristic samples, which were the CF90, CF110 and

CF150 samples, as detailed later discussed. It should be noted that CF110, CF120, CF130 and CF140 demonstrated almost similar results in terms of decomposition.

Figure 2 outlines the methods of sample preparation, weathering, recovery, and characterisation. These characterisation methods are detailed in the following chapter.

Differential scanning calorimetry

Differential scanning calorimetry (DSC) was carried out with a DSC-Q2000 device from TA Instruments (New Castle, DE, USA) to find the appropriate curing temperature. The analysis of pre-pregs was carried out using specimens with a mass ranging from 5 to 8 mg, heated at a ramp rate of 10 °C/min from room temperature to 200 °C in a nitrogen environment with a flow rate of 50 mL/min.

Mass of the samples after ageing and decomposition

In this study, the decomposition percentage of CFRP was analysed. The cured CFRP was weighed. The mass of the epoxy component within the CFRP (uncured pre-preg) samples was estimated to be 30 mass% of the total CFRP.

After exposing the CFRP samples to UV radiation (with each sample containing three layers of carbon fibre), their mass was measured. The mass of the fibres recovered by H_2O_2 at different temperatures was also measured. The decomposition (De) of the matrix in terms of the weight ratio [%] was calculated. Based on the mass measurements, we chose the CF90, CF110, CF130, CF140 and CF150 samples for further characterisation.

Scanning electron microscopy

The morphology of CF90, CF110 and CF150 was acquired by scanning electron microscopy (SEM). A Zeiss SEM5000 (Hilden, Germany) was used to examine the surface morphologies at an 8 kV accelerating voltage upon applying a platinum-coated conductive layer to the samples. Even though carbon fibre is conductive, we applied it because the epoxy traces are not. A sample exposed only to UV was measured with A JEOL JSM-6380 (Tokyo, Japan) SEM at an accelerating voltage of 5 kV. We applied gold sputter coating to enhance the conductivity before placing them into the specimen chamber.

X-ray diffraction

To assess the crystallinity of the recycled carbon fibres, we carried out X-ray diffraction (XRD) measurements on the CF90, CF110 and CF150 samples. For this purpose, an X-ray diffractometer X'pert PRO from PANanalytical (EA Almelo, The Netherlands) was used. The operating voltage was 45 kV, the current was 40 mA, the scanning rate used was 0.011°/min, and it was operated in the wide-angle ($2\theta = 10$–$90°$) range.

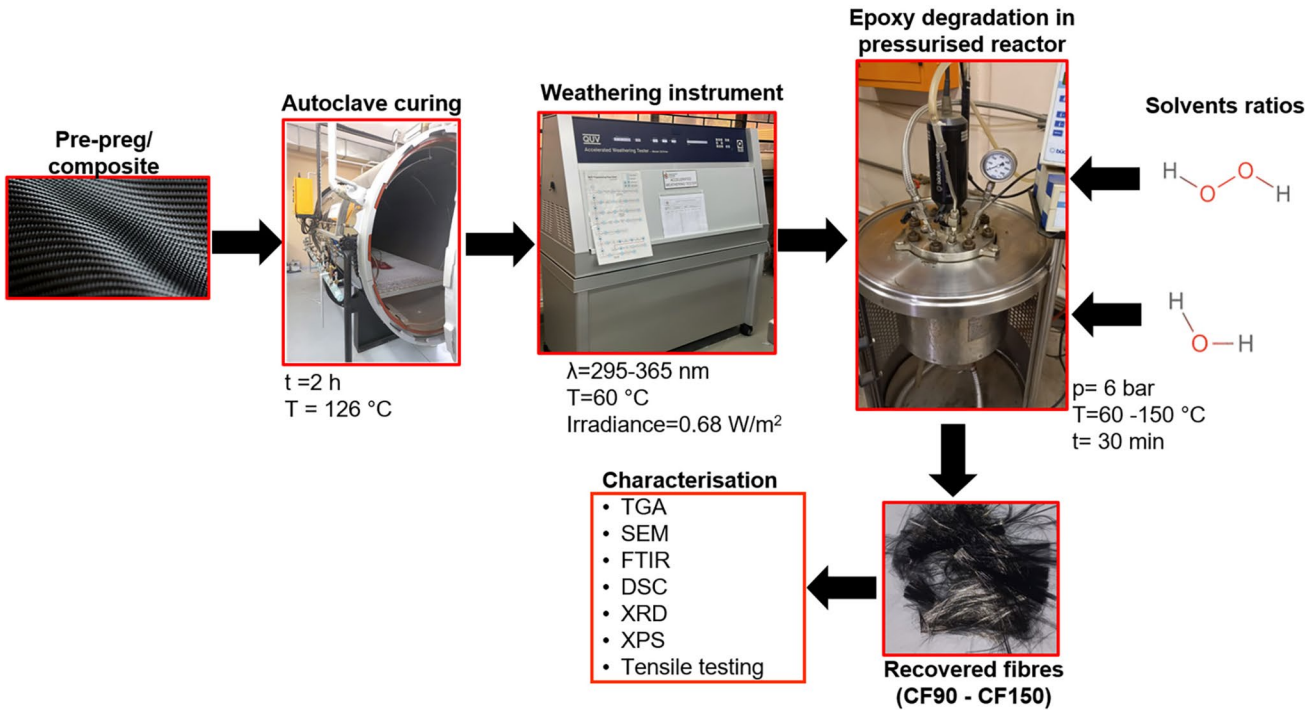

Fig. 2 Schematic diagram of the carbon fibre recovery preparation

Fourier-transform infrared spectroscopy

To determine the impurities present in the samples and to evaluate the decomposition of the epoxy resin a Fourier-transform infrared (FTIR) spectrometer from Perkin Elmer (Spectrum 100; Branford, CT, USA) was used with a wavelength range of 600–4000 cm^{-1}, with a resolution of 4 cm^{-1}. A total of 32 scans were collected for the chosen uncured prepreg reference sample and for the CF90, CF110, and CF150 samples.

Thermogravimetric analysis

To determine the mass loss due to temperature thermogravimetric analyses (TGA), using a Perkin-Elmer STA 6000 (Shelton, United States of America) device was carried out. For this purpose, samples with an initial mass of 10–12 mg were measured with a heating ramp rate of 10 ℃·min^{-1} from 50 ℃ to 1000 ℃ and in a 100 mL·min^{-1} volume rate nitrogen purge flow.

X-ray photoelectron spectroscopy (XPS)

XPS spectra were collected using a Thermo Fisher Nexsa G2 XPS System utilising an Al Kα source (15 kV, 60W). All the spectra were calibrated concerning the aliphatic C–C peak binding energy at 284.8 eV. The curves were fitted using the CasaXPS software version 2.3.25 with a combined Gaussian–Lorentzian profile after subtracting the background.

Single fibre tensile tests and statistical analysis

To characterise the mechanical properties of the recovered material, we decided to carry out tensile tests on single fibres. Since CF150 performed the best among the samples, we chose to use that one for testing its mechanical properties. The other samples were less pure and contained significant traces of epoxy resin. These impurities likely interfered with the ability to separate the individual fibres for detailed analysis.

As a reference sample, we took fibres from the uncured pre-preg and tested those. The pre-impregnated carbon fibres were immersed in acetone to wash away the uncured epoxy from the fibres. This process allowed for a clear comparison of the mechanical properties between the virgin carbon fibres (neat CF) taken from the uncured prepreg and the CF150.

We cut paper frames with a manual punching machine. The frame was 40 × 20 mm with a window size of 25 × 10 mm, where 25 mm corresponds to the gripping length. We fixed a single fibre into the frame with pieces of adhesive tape. The diameter of the fibres was then measured by an Olympus BX51M (Hamburg, Germany) optical microscope equipped with a digital camera and imaging system. The diameter of each fibre was measured at 3 places in its middle section.

A Zwick Z005 (Zwick GmbH., Ulm, Germany) universal load machine equipped with a 20 N load cell and a single fibre gripping unit with small rubber jaws was applied for the tensile tests. We gripped the paper frame and then cut the edges prior to testing. Hence, only the fibre remained between the grips. The gripping length was 25 mm, while the test speed was 2 mm/min. We tested 15–15 individual fibre specimens for both recycled and virgin fibres.

We compared the tensile strength, tensile modulus and elongation at break of the two types of specimens by statistical analysis. We carried out an *F*-test to see if the standard deviations can be considered the same, and then, the Student's paired two-sample *t*-test was used to see if the averages of these values can be regarded as different.

Results and discussion

Differential scanning calorimetry (DSC) of the composite laminates

DSC analysis was conducted to investigate the thermal characteristics of the uncured CFRP, as depicted in Fig. 2. The primary objective of this analysis was to determine the appropriate curing temperature for the preparation of specimens that would be subjected to a comparative test between recycled and virgin carbon fibres. Figure 3 shows the DSC plot of the pre-pregs.

The DSC data plot for uncured pre-pregs shows a broad exothermic peak highlighted in Fig. 3. This peak is due to the curing of the CFRP composite's epoxy resin, which is a chemical reaction that crosslinks the epoxy molecules, resulting in a solid material. The curing process of the material begins at around 110 °C, as indicated by the onset temperature of the curing peak. The curing process reaches its peak at around 150 °C and is completed at about 180 °C, as indicated by the end of the exothermic peak. The total enthalpy change of the curing reaction is approximately 60.33 J/g. In this study, the chosen curing temperature was 125 °C and the curing time of 2 h to allow a gentle curing.

The decomposition rate of the matrix

To simulate the ageing of composites and examine the impact of UV and water exposure, CFRP samples were subjected to UV radiation and water vapour. The resulting weight loss decomposition values are given in Table 1.

The average weight loss due to decomposition of the composite panels after UV exposure was 0.88%, with a standard deviation (STD) of 0.06%. UV radiation led to the reduction

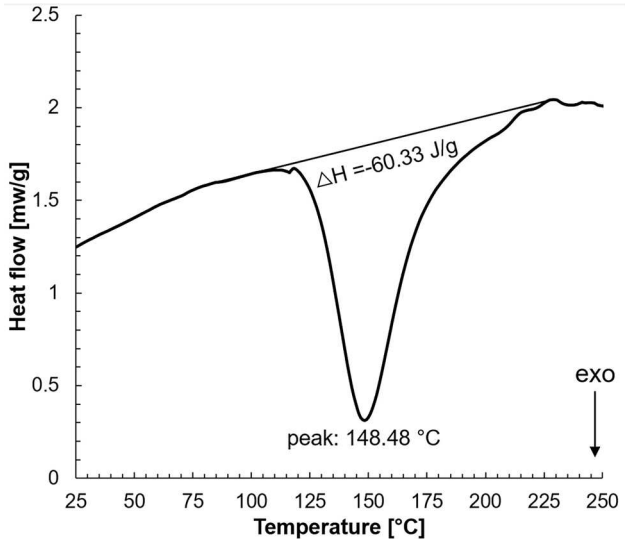

Fig. 3 DSC of the pre-preg

in mass for the CFRP samples. Although, UV radiation has the capacity to decompose the epoxy matrix in CFRPs, the observed decomposition levels were relatively low. UV mainly has an effect close to the surface, and CF also does not let it penetrate deep. During the lifespan of such composite panels, we cannot expect a significant decomposition due to weather. In the calculations, we still took this minor change into account the way that aging affected the matrix only.

On the other hand, as expected, the H_2O_2 treatment in the reactor decomposed the matrix, and the reactor's temperature had a significant effect. We had 3 distinctive groups of the specimens by means of the residual mass. Samples at and below 90 °C had hardly any decomposition of the matrix. Samples at 100–140 °C had a moderate decomposition, and the sample at 150 °C had close to complete decomposition. Based on these observations, we selected CF90, CF110, CF130, CF140, and CF150 for further detailed testing and discussion. As highlighted in Fig. 4, these temperatures showed significant decomposition. A similar study was conducted by Xu et al., which aligns with our findings [19]. They used a mixture of hydrogen peroxide and N, N-dimethylformamide to break down epoxy matrices and achieved a 95% decomposition ratio at 160 °C. The decomposition ratio of CF150 is about 93%, as highlighted in Table 1 and Fig. 4, considering the 93% decomposition observed, it is recommended to explore test temperatures reaching up to 160 °C. According to Wang et al. [28], the optimal temperature range for achieving a favourable decomposition ratio extends from 160 °C to 180 °C. It is crucial to acknowledge that elevating the temperature not only intensifies the decomposition process but also leads to an increase in pressure. This escalation in pressure poses potential safety concerns, which are contingent upon the specific type and quality of the reactor utilised.

Morphological properties

Scanning electron microscopy (SEM) was employed to determine the presence of any remaining resin residue. The recovered carbon fibres exhibited a clean and smooth surface after treatment, devoid of ridges or holes, as depicted in Fig. 5a–c. CF90 displayed minor decomposition with epoxy resin observed on the fibre surface. Table 1 and Fig. 4 show a decomposition rate of approximately 51% at 110 °C, which is also evident in the CF110 image where partial decomposition occurred. CF150 samples revealed only a few spots indicating micron-sized epoxy resin residues on the fibre surface. Overall, the recycled fibres exhibited minimal impurities on their surfaces, remained largely spotless, and

Table 1 Sample masses and decompositions

Sample	Mass after curing [g]	Estimated epoxy content [g]	Mass upon weathering [g]	Decomposition by weathering [%]	Mass of recovered CFRP [g]	Mass difference [g]	Decomposition of the matrix [%][e]
CF60	4.468	1.340	4.426	0.94	4.410	0.016	1.2
CF70	4.539	1.362	4.498	0.90	4.418	0.079	5.9
CF80	4.559	1.368	4.523	0.79	4.423	0.099	7.3
CF90	4.476	1.343	4.435	0.92	4.337	0.098	7.4
CF100	4.696	1.409	4.653	0.92	4.184	0.468	33.5
CF110	4.643	1.393	4.602	0.88	3.908	0.693	50.2
CF120	4.654	1.396	4.612	0.90	3.967	0.645	46.6*
CF130	4.653	1.396	4.611	0.903	3.918	0.693	51.2
CF140	4.672	1.402	4.630	0.899	3.861	0.769	54.1
CF150	4.548	1.364	4.512	0.79	3.247	1.264	93.4

*Sample CF120 has exhibited a deviation in its peak performance trend, which may be attributed to the inhomogeneity of the specimen

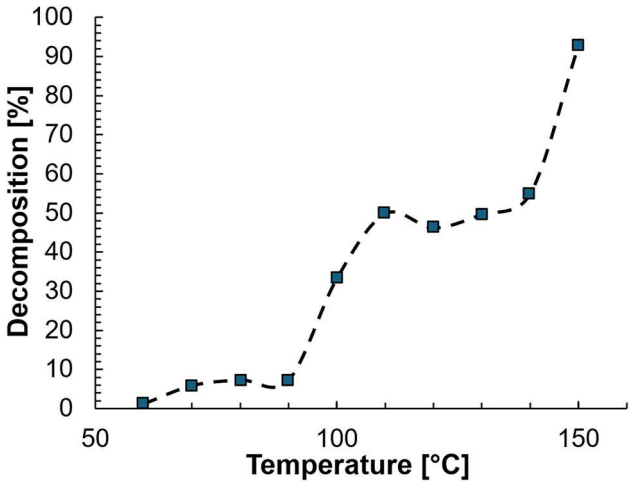

Fig. 4 Weight loss due to recovery

showed no signs of fibre damage. These findings suggest that the epoxy resin underwent successful oxidation and decomposition, resulting in its effective removal from the fibre surface at 150 °C and a pressure of 6 bar. Figure 5d revealed visible cracks in the epoxy matrix, likely resulting from prolonged UV exposure. These cracks indicate the degradation and breakdown of the polymer structure under UV. Table 1 further demonstrates a resin decomposition rate of about 90% with the resulting impurities (Fig. 5a–c).

Physico-chemical properties

The XRD spectra of the virgin carbon fibres (neat CF), uncured pre-preg and recovered fibres (CF90, CF110, CF130 CF140 and CF150) were determined to characterize the structural changes. Understanding the extent of structural damage is crucial in assessing the feasibility and suitability of utilizing recycled carbon fibres in various applications. Figure 6 shows the spectra obtained. The XRD plots were studied and the 2Θ angle was accurately evaluated from the

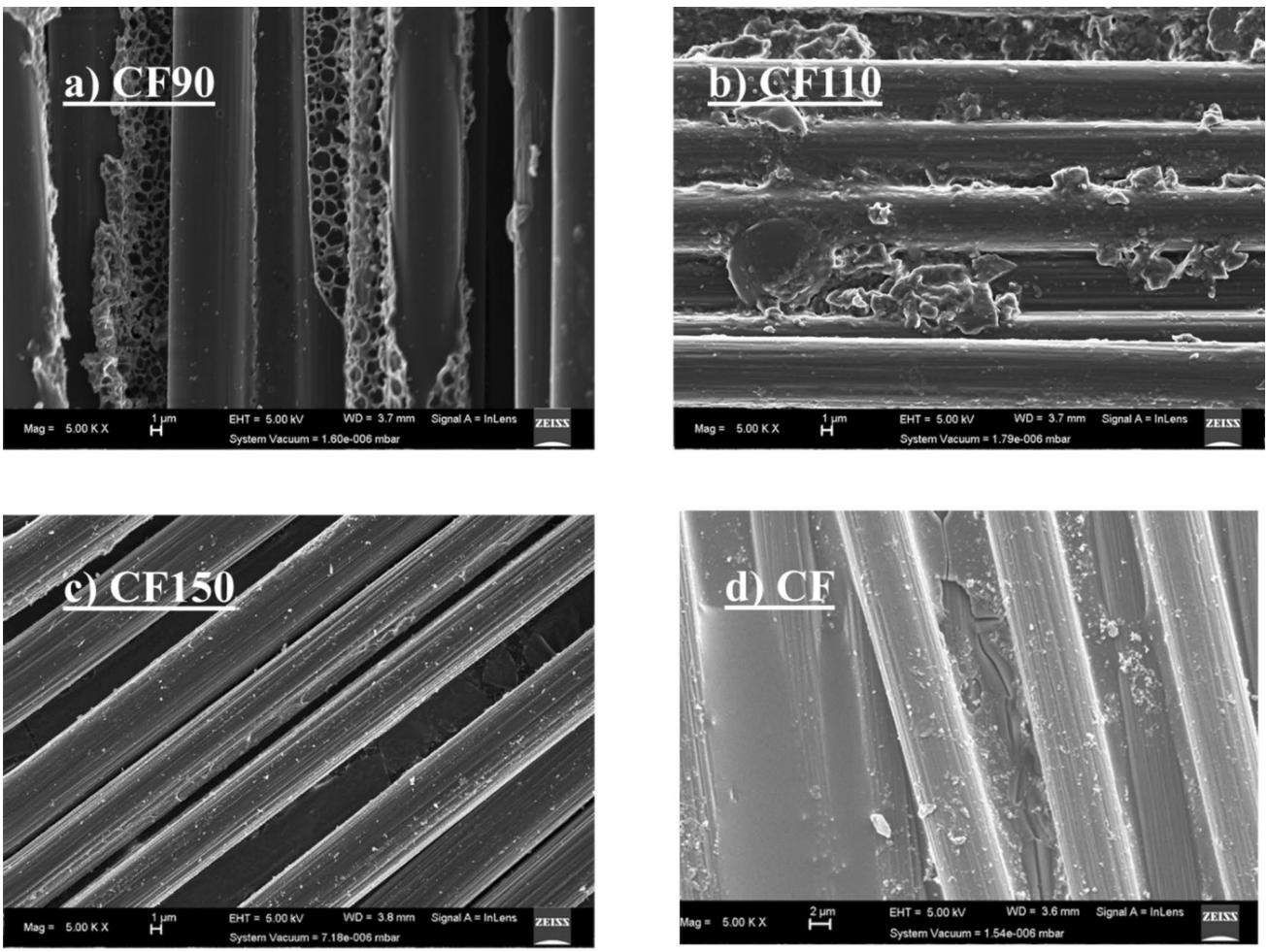

Fig. 5 SEM images of recovered fibres: **a** at 90 °C, **b** at 110 °C, **c** at 150 °C, **d** carbon fibre laminate after UV exposure, prior to recovery

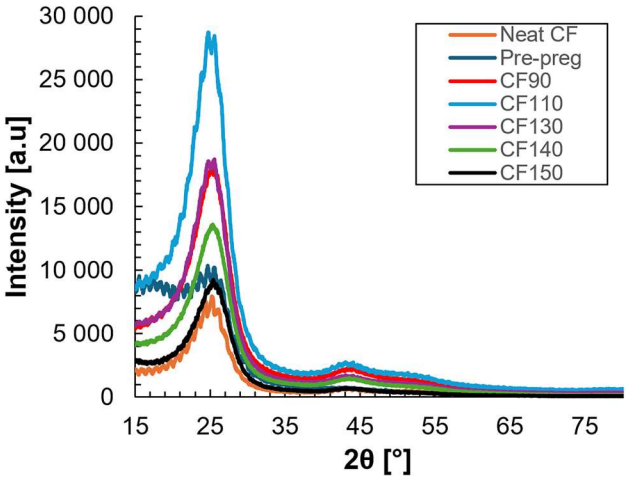

Fig. 6 XRD spectra of neat CF, pre-preg and CFRPs

002 plane. The interlayer d-spacing $d_{(002)}$ value was calculated using Bragg's law. The full width at half maximum (FWHM) was calculated, and the crystallite size (L_c) was derived from 002 plane reflection through the Debye–Scherrer formula [29].

Lastly, the degree of graphitization was determined. The degree of graphitization (D_g) refers to the extent to which carbon material, such as graphite or carbon fibre, has achieved a graphitic structure. It measures the ordering and the arrangement of carbon atoms in the material (1):

$$D_g = \frac{L_c}{d_{(002)}} \tag{1}$$

where L_c is the crystallite size and $d_{(002)}$ is the spacing of the graphite layers. L_c in (1) can be calculated as follows (2):

$$L_c = \frac{k \times \lambda}{\beta \times \cos\theta} \tag{2}$$

in which k represents the Scherrer-constant (0.98), λ denotes the wavelength (1.54), β denotes the full width at half maximum (FWHM).

As indicated in Fig. 6, the neat CF (purple) exhibits the most intense and well-defined peaks, indicating a high degree of crystallinity due to the absence of processing that could disrupt its crystal structure. The CF150 (black) displays slightly less intense and broader peaks than the neat CF, suggesting that the high-temperature (150 °C) recovery process in the autoclave reactor has somewhat disrupted the crystallinity carbon fibre. The uncured prepreg (green) manifests even broader and less intense peaks than the CF150 sample, likely due to additional components like resin and curing agents, which may interfere with the carbon fibres' packing in the composite material. Both CF90 (blue) and CF110 (red) samples exhibit peak patterns similar to CF150, indicating that lower recovery temperatures (90 °C and 110 °C) have a comparable effect on the crystallinity of carbon. The crystallinity peak profiles of CF130 and CF140 closely resembled those of CF110, as anticipated given their nearly identical decomposition rates. The broad peaks around the lower 2θ values (e.g., 20–30°) further indicate the presence of some disordered, amorphous phases in the sample.

Table 2 Summary of the degree of graphitization results of carbon fibres treated under different conditions

Sample	2θ [°]	$d_{(002)}$ plane [nm]	FWHM [nm]	L_c [nm]	Degree of graphitization [−]
CF90	25.307	0.352	3.5	2.4	6.9
CF110	24.715	0.360	3	2.8	7.9
CF130	24.712	0.35	3	2.7	7.9
CF140	24.713	0.36	3	2.8	7.8
CF150	25.391	0.351	3	2.8	8.1
neat CF	25.222	0.352	2.5	3.4	9.5

XRD curves exhibited 2Θ angles around 25°, corresponding to the 002 plane, as indicated in Table 2. The CF150 samples that were recovered had a degree of graphitization of 8.1, with stacked crystallite layers found to be comparable to those of the virgin CFs (which were extracted from the uncured prepreg by washing with acetone), which had a degree of graphitization of 9.5 (Table 2). These findings indicate that the recovered carbon fibres maintain a high level of graphitization, similar to that of virgin carbon fibres.

The decrease in the degree of graphitization observed in CF150 can be attributed to various factors associated with the recycling process. Although, the underlying mechanisms are intricate and may vary depending on specific conditions and materials, several plausible reasons contribute to this reduction. First, during the recovery process using hydrogen peroxide, the carbon fibres are exposed to an oxidative environment. This exposure results in the introduction of oxygen-containing functional groups on the carbon fibre surface and close to the surface, which might have disrupted the graphitic structure and consequently reduced the degree of graphitization. Second, the hydrogen peroxide treatment aims to decompose the epoxy resin that binds the carbon fibres in the composite material. This resin decomposition process can introduce impurities and defects into the carbon fibres, leading to a decrease in the degree of graphitization. Moreover, the recycling process can induce defects and disruptions in the crystal lattice of the carbon fibres, affecting their degree of graphitization. These induced defects act as stress concentrators, further influencing the mechanical properties of the fibres.

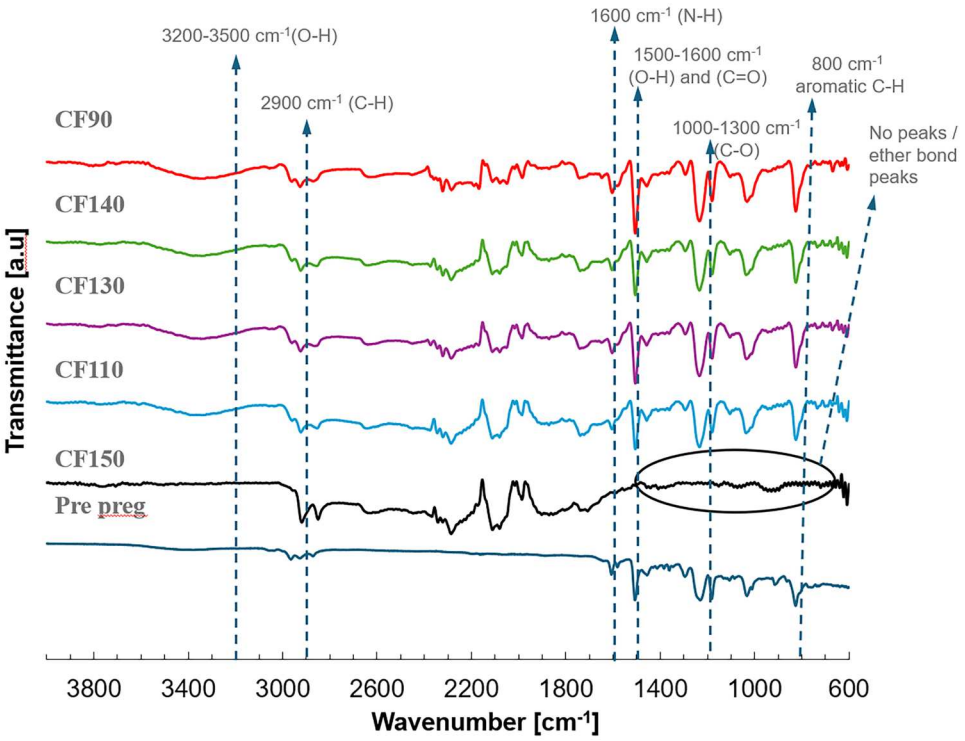

Fig. 7 FTIR spectra of the test samples

Figure 7 depicts the results of the FTIR spectra of the recycled carbon fibres and the uncured prepreg. Since FTIR is not sensitive to C–C symmetric bonds, any bands observed in the recovered carbon fibre's FTIR spectrum can originate from imperfect carbonization of the precursor or most importantly, epoxy resin residue that was left over from the recovery process.

The recovered carbon fibres typically display absorption bands at 1000 cm^{-1} which correlates to the C–O vibration bonds, 1300 cm^{-1} which correlates to the C=O bonds from the carboxylic acid functional groups, and 1500 cm^{-1} which correlates to the N–H bonds for an amine functional group (Fig. 4b). Vinyl group C–H bonds correlates to 3000 cm^{-1}. The degradation of the epoxy resin during the recovery process exposes these groups. Additionally, CF150 demonstrated a baseline from about 800 to about 1800 cm^{-1}. The results obtained are similar to the ones reported by Deng et al. [30, 31].

Ether and carboxylic groups of the epoxy were broken down during the recovery process, they formed during the oxidation of the epoxy resin. The absence of carbonaceous deposits and any visible flaws on the fibre surface indicates a good recovery from the recycled CF. These carbonaceous deposits are C–O and C=O bonds.

XPS analysis was carried out to see changes in the surficial chemical composition due to the weathering and recovery process at different temperatures. The CFRP sample is the inside of the matrix in which case a fibre layer was separated from the panel and the inner side was analysed. Survey spectra of the samples and composition can be seen in Fig. 8 and Table 3, respectively. All samples have similar compositions with only minor differences. The neat CF sampled from the prepreg and washed with acetone has higher *O* and *N* content probably because

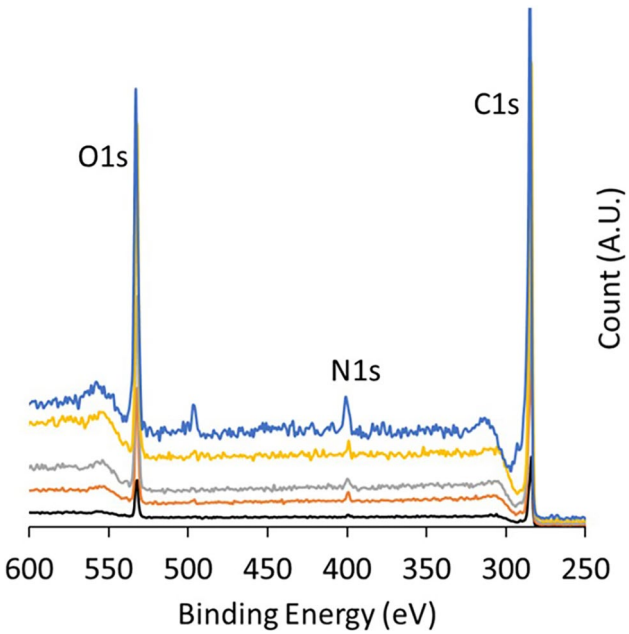

Fig. 8 XPS survey spectra of neat CF (black), CFRP (orange), CF90 (grey), CF110 (yellow), CF150 (dark blue). Spectra are displaced for better visualization

Table 3 XPS survey data of the carbon fibre samples

Sample	At%		
	C1s (284 eV)	O1s (532 eV)	N1s (399 eV)
neat CF	81.34	17.04	1.62
CFRP	79.52	17.24	3.24
CF90	74.58	23.26	2.16
CF110	76.93	21.73	1.34
CF150	73.92	21.78	4.30

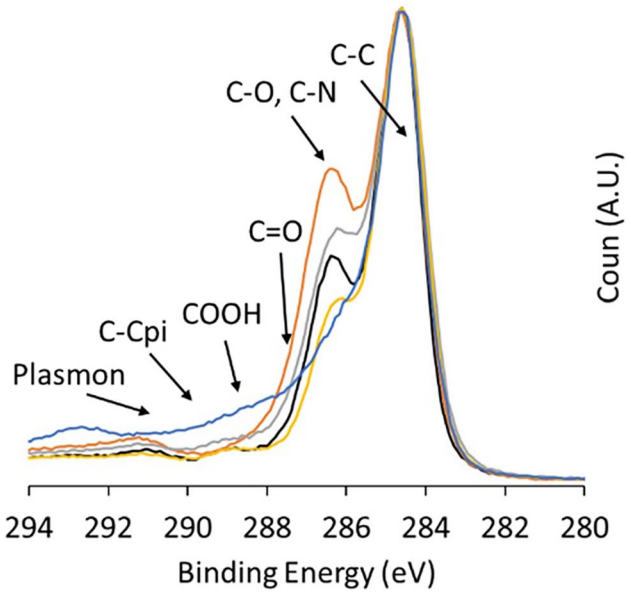

Fig. 9 XPS C1s normalized spectra of neat CF (black), CFRP (orange), CF90 (grey), CF110 (yellow), CF150 (dark blue)

washing was not perfect, there could be some residues of epoxy resin on the surface.

There is a higher *C* and *N* content in the CFRP sample compared to the neat CF sample due to the presence of epoxy resin in the matrix. The survey data of the recovered samples (CF90, CF110 and CF150) seems to be similar with also small differences. In all cases, the *O* content is higher compared to neat CF and CFRP suggesting either remnants of resin or oxidized carbon fibres in the sample. However, the *N* content seems to rise with treatment temperature (excluding CF110).

C1s high-resolution spectra were taken of the samples as well (Fig. 9 and Table 3). Deconvolution was not carried out to minimize the possibility of errors due to the complexity of the method and the system as suggested by Major et al. [32]. Parts of the C1s spectra were labelled based on the work of Weitzsacker et al. [33] and Oishi et al. [34, 35]. All the samples have similar spectra and composition with only the CF150 sample standing out (Fig. 9). The C1s of neat CF (sampled from the uncured pre-preg and then washed by acetone) does not look like neat CF since it has a considerable amount of *O* and *N*-related bonds on the surface leading to the conclusion that its recovery from the pre-preg was not perfect [33]. The CFRP sample looks similar with a higher C–O, C–N peak marking the presence of the epoxy matrix in the system. In the recovered CF samples, we can observe the C–O, C–N peak going down with rising treatment temperature. In the case of CF150, its line shape is most similar to Weitzsacker et al.'s work [33] whom analysed pristine carbon fibre.

To assess the weight loss of CFRP and recycled CFs, a TGA analysis was conducted (Fig. 10). As the temperature increased, there was a gradual decrease in sample weight. However, under a nitrogen atmosphere the neat CF curve stayed the same from 50 °C to 850 °C in the TGA curve,

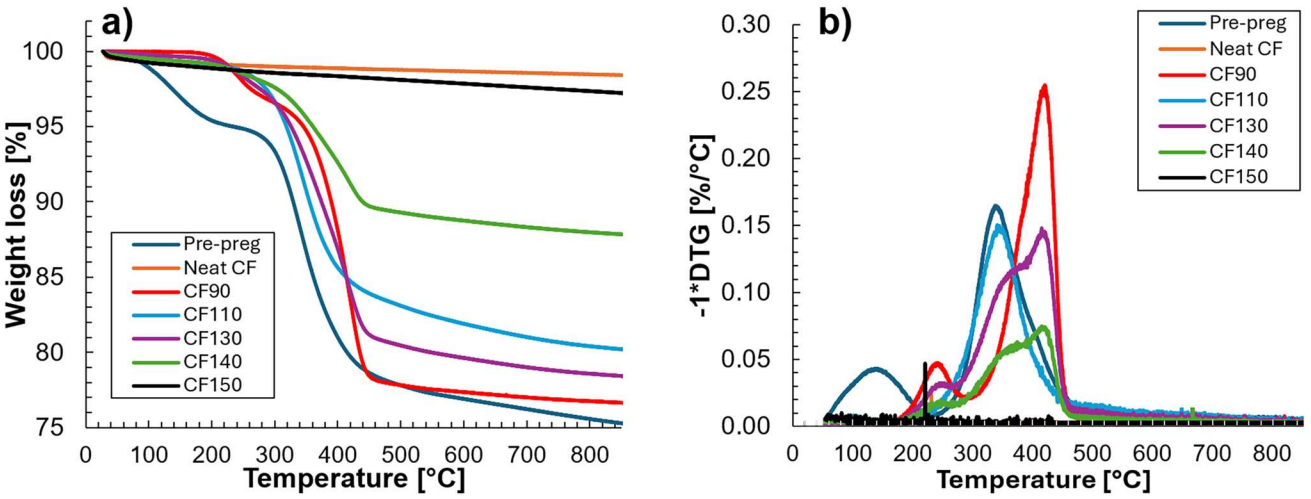

Fig. 10 **a** TGA and **b** DTG curves of neat and recovered carbon fibre samples

with no peaks observed. This suggests that carbon fibre does not decompose under these temperatures, aligning with TGA results reported by Deng et al. [30].

According to Table 1, CF150 exhibited a decomposition percentage of approximately 93%. CF150 displayed a weight loss of around 5%, indicating successful decomposition of the epoxy resin using hydrogen peroxide. Examining the data provided by CMT for carbon fibre, it indicates an epoxy resin content of approximately 30%.

Figure 10b represents the DTG (derivative thermogravimetric) curve, showing the rate of mass loss during the thermal decomposition of recovered carbon fibres treated with hydrogen peroxide at various temperatures (from 90 °C to 150 °C, labeled CF90 to CF150).

The tests on CFRP samples via TGA revealed a notable 25% mass reduction from the initial mass. We predicted a 30% decrease in weight because the nominal epoxy content is 30% of the pre-preg laminate. Based on the TGA results, in the case of CF90, the decomposition percentage was approximately 8%. That is in agreement with the data in Table 1 (7.5%).

Similarly, CF110 exhibited a decomposition percentage of around 50% according to Table 1. The TGA results showed that approximately 30% of the sample underwent decomposition. This discrepancy in results may be attributed to the non-uniform distribution of epoxy resin on the fibre surface during the collection of the 10 mg sample. Even though the trends are clear, these findings highlight the importance of considering the homogeneity of epoxy resin distribution when evaluating weight loss and decomposition percentages in TGA analysis.

The peaks in the DTG curves indicate the temperatures where the most significant decomposition occurs. In the DTG analysis, the pre-preg itself shows a broad decomposition peak around 350–400 °C, indicating a single major degradation event due to the breakdown of the epoxy matrix. Additionally, there is an initial peak at 150 °C, hydroxyl groups (OH) from the epoxy resin or hardener can release water molecules as the temperature increases. We suspect this was the evaporation of OH molecules at the first peak.

For CF90, a similar broad peak appears at 350–400 °C, but with a slightly reduced rate of mass loss. The first peak shifts to 250 °C, revealing two distinct degradation mechanisms at this treatment temperature. CF110 displays a peak between 300 and 350 °C, similar to the pre-preg, but the 150 °C peak disappears, indicating a single degradation mechanism. CF130 exhibits two peaks, with the first being more prominent and occurring at a lower temperature compared to CF110, suggesting a faster decomposition of the epoxy matrix. The second peak is less pronounced. CF140 shows a pattern similar to CF130, but with a lower rate of mass loss for the first peak, indicating a more efficient breakdown of the matrix. Lastly, CF150 follows a trend similar to CF, demonstrating minimal decomposition, which suggests that both samples are highly pure. CF150 shows minimal mass loss, indicating greater thermal stability compared to the other samples.

Kinetics study

The Arrhenius equation, which correlates the rate constant (k) with temperature (T), was applied to our decomposition data in Table 1 to investigate the influence of kinetics on epoxy degradation [36]. This was accomplished using Eq. 3:

$$\mathrm{k} = A \cdot e^{\left(-\frac{E_a}{RT}\right)} \tag{3}$$

where: A is the pre-exponential factor, E_a is the activation energy, R is the universal gas constant (8.314 J/mol K), T is the temperature in Kelvin.

To ascertain the rate constant, we assumed that the decomposition reaction of hydrogen peroxide with the epoxy resin reinforced with carbon fibre follows first-order kinetics, represented by the following formula [36], (4):

$$k = -\frac{1}{t}(1 - \mathrm{De}) \tag{4}$$

where: t is 1800s, De is the extent of decomposition [%].

Following the computation of the rate constant using the decomposition percentages of each sample indicated in Table 1 and Fig. 11, we plotted ln(k) against 1/T using the data reported in Table 4. The subsequent table represents the relationship between 1/T and ln(k) to calculate the activation energy (E_a), with the slope obtained being multiplied by the universal gas constant (R). From the graph, the slope was determined to be 7630.9, resulting in an activation energy of 63.4 kJ/mol.

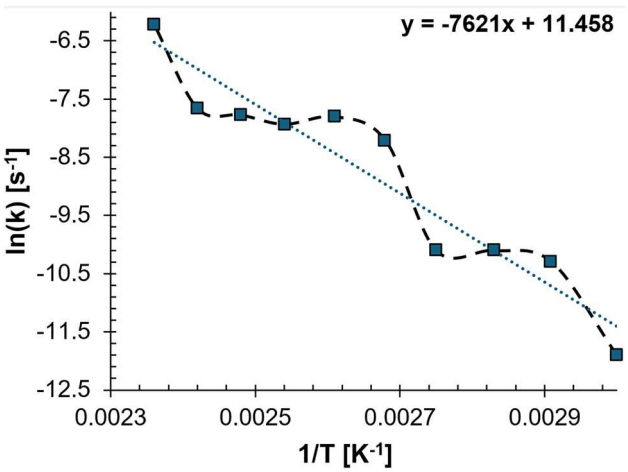

Fig. 11 Activation energy graph

Table 4 1/T *vs* ln(k)

Sample	T (°C)	1/T (K^{-1})	ln(k) (s^{-1})
CF60	60	0.003	− 11.91
CF70	70	0.00291	− 10.31
CF80	80	0.00283	− 10.1
CF90	90	0.00275	− 10.08
CF100	100	0.00268	− 8.21
CF110	110	0.00261	− 7.8
CF120	120	0.00254	− 7.93
CF130	130	0.00248	− 7.77
CF140	140	0.00242	− 7.66
CF150	150	0.00236	− 6.22

Table 5 compares the decomposition processes of carbon fibre-reinforced polymers (CFRPs) using hydrogen peroxide (H_2O_2) and pyrolysis.

Partial environmental impact

Our experimental findings, substantiated by literature [40], strongly support the use of hydrogen peroxide as an environmentally friendly method for decomposition. The data presented in Table 6 clearly demonstrate the efficacy and sustainability of this approach compared to thermal treatments.

Mechanical properties

Tensile stress–strain curves of virgin and recycled single carbon fibres are shown in Fig. 12 whereas data are collected in Table 7. The testing process involved conducting a total of 15 test runs for both the CF150 and the neat CF samples. It is evident that UV irradiation, as reported elsewhere in the literature [25], might damage the fibres by partial degradation. The graphitic structure is less perfect, which could cause weakening if the mechanical properties, as reported in Table 7.

Table 5 Comparison of recovery by hydrogen peroxide and pyrolysis

Parameter	H_2O_2 decomposition (this study)	Pyrolysis
Kinetics	Decomposition follows first-order kinetics with activation energies of 63.4 kJ/mol (see Fig. 10 and Table 4)	Follows first-order kinetics with activation energies between 150 and 200 kJ/mol due to high-temperature [37]
Reagent consumption	To treat 192 tons of CFRP 212.9 cubic meters of hydrogen peroxide are required. This amount was calculated based on the stoichiometric reaction between hydrogen peroxide and the Bisphenol component in the CFRP	No chemical reagents are required other than inert gases (e.g., nitrogen) for maintaining an oxygen-free environment Lower operational costs related to reagent consumption [38]
Energy input	Moderate energy input due to the exothermic nature of H_2O_2 decomposition. Temperatures generally range between 60 and 150 °C Lower energy consumption compared to pyrolysis	High energy input is needed to maintain temperatures between 400 and 700 °C. Energy consumption is higher due to heating requirements and inert gas usage [39]
Quality of recovered products	High-quality, non-fragmented, long carbon fibres with minimal surface damage	Carbon fibres can be damaged or oxidized at high temperatures Surface defects and reduced mechanical properties of the recovered fibres [14]

Table 6 Differences between chemical and thermal treatments in terms of wastewater generation, energy consumption, and CO_2 emissions

Criteria	Chemical treatment (Hydrogen peroxide)	Thermal treatment
Wastewater generation	High (large volumes of wastewater with residual chemicals). However, this waste can be treated to produce other useful organic compounds that the market requires [40]	No wastewater generation [40]
Energy consumption	Low to moderate. In this study, we use low temperature	High due to high-temperature usage
CO_2 emissions	Low [40]	High due to the combustion method [41]
Environmental impact	Potential contamination due to wastewater disposal	Contributes to global warming due to CO_2 emissions (Pyrolysis is associated with 2.9 kg CO_2 eq/kg CFRP waste) [42]

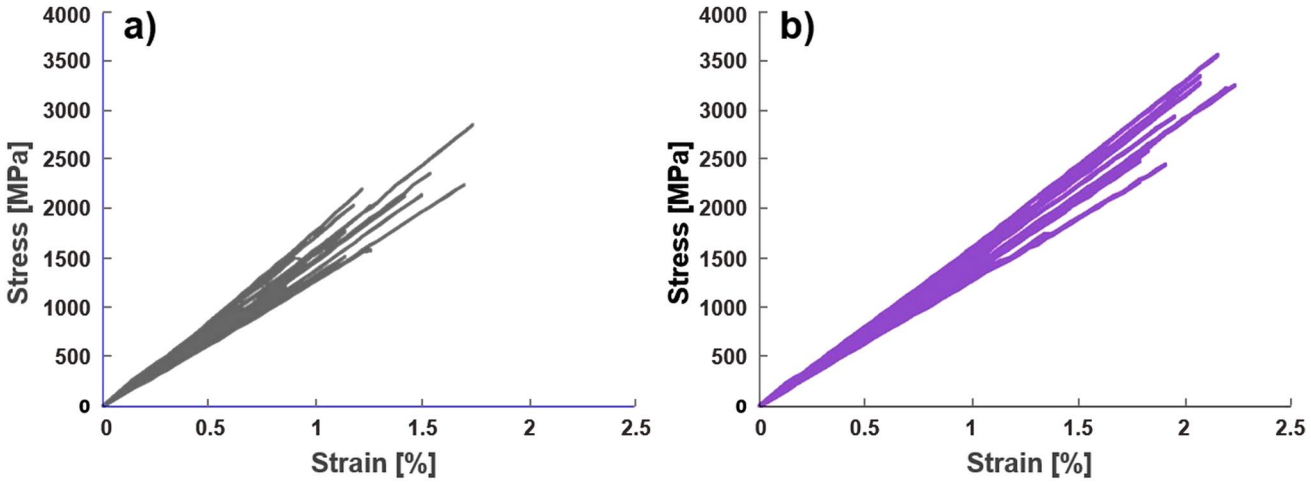

Fig. 12 Tensile stress–strain curves of single carbon fibres: **a** CF150, **b** neat CF

Table 7 Mechanical properties results in comparison with works from literature

Sample	Young's modulus [GPa]	Elongation at break [%]	Tensile strength [MPa]
CF150	143.11	1.29	1893
STD	17.88	0.22	433
neat CF	146.15	1.88	2795
STD	12.02	0.24	423
Change	− 2%	− 31.4%	− 32.2%

In this specific case, we decided to utilize a treatment involving a temperature of 150 °C, which might have resulted in superior decomposition percentages.

However, it is important to note that such a high temperature might have had an adverse effect on the tensile stress, causing a decrease when compared to the virgin single fibre samples [43]. Carbon fibres are susceptible to surface scratches and abrasions, which can lead to a deterioration of properties like strength [44]. Additionally, it is worth mentioning that the only scratches and abrasions in most cases can be attributed to the use of an agitator [45], which was used in the recovery process. Furthermore, the agitator could fragment or damage the fibres that are very rigid.

Lastly, the slight decrease in tensile stress observed in the recycled fibre aligns with the XRD results, indicating a significant decrease in the degree of graphitization, suggesting that the recovered fibres may have experienced a slight compromise in their mechanical properties.

According to the data presented in Table 7, a comparison between recycled carbon fibre and virgin carbon fibre reveals some interesting characteristics.

Notably, the treatment of carbon fibres with hydrogen peroxide during the recovery process does not appear to have caused any damage or disruption to CF150's microstructure concerning its stiffness, as Young's modulus remains unaffected. Note that we did not measure the elongation by optical ways; we calculated it from the displacement of the machine crosshead. The real modulus values of the fibres are likely higher than what we obtained. The results, on the other hand, are suitable for comparing the modulus of the virgin and the recovered fibres, which seem to be the same value.

When we consider tensile strength, CF demonstrates a significantly higher value at 2776 MPa, while CF150 exhibits a lower tensile strength of 1807 MPa. Additionally, neat CF and CF150 display an elongation value of nearly 2% and 1.3%, respectively.

We compared reference neat CF and CF150 fibres by means of the variance of their tensile modulus, tensile strength, and elongation at break, respectively, by *F*-test. The variance of the two sets can be considered the same for all three different parameters tested. The *F*-value was 0.14, 0.70, and 0.69 for the tensile moduli, tensile strengths, and elongations at the break, respectively, all being greater than 0.05.

Based on this finding that the variances are equal, we carried out a set of two-sample Student's *t*-tests to compare the averages of the two materials for the same parameters. We consider the effect of the recovery process significant on a certain property if the *p*-value is smaller than 0.05.

As a result of the *t*-tests, we obtained that the modulus of the virgin and recovered fibres can be considered equal ($p = 0.59 > 0.05$). The elongation at break and the tensile strength decreased significantly, $p = 6.2 \times 10^{-6}$ and $p = 2.6 * 10^{-6}$. This means that the ageing and recovery did not affect the modulus of the carbon fibres, but their strength and elongation at break decreased greatly. That indicates structural damage within the fibres, which makes local faults within

the microstructure. The recovered fibres have the same characteristic, but are prone to fail earlier due to earlier crack initiation from these zones.

The properties of the recovered fibres are still fair for making new composites, and better than those of glass or basalt fibres. These recovered carbon fibres can be good alternatives to glass fibres because they have a smaller density (1.8 *vs.* 2.6 g/cm^3), a similar tensile strength, and a much higher modulus.

Conclusions

This study aimed to explore possible ways for recycling carbon fibres from prepreg-based composite panels. We used hydrogen peroxide, which is an eco-friendly alternative for chemical recovery. We aged the composite laminate samples at elevated temperature, high humidity and high UV irradiation for 1000 h to simulate the lifespan of the composite panels. The ageing did not cause significant degradation of the resin. We investigated the effect of the recovery temperature within the range of 60–150 °C and found that temperatures above 110 °C cause a significant decomposition of the resin within 30 min.

Through TGA analysis, we observed changes in the mass of the recovered samples. Notably, CF150 exhibited successful epoxy resin decomposition, while CF90 and CF110 displayed lower decomposition percentages, potentially attributed to the low energy and the non-uniform resin distribution.

The absence of carbonaceous deposits and visible flaws on the surface characterized by SEM and XPS indicated a successful recovery process. However, XRD analysis indicated minor structural damage in the recycled fibres, suggesting that some level of structural alteration occurs during the recycling process. The modulus and the characteristics of the tensile curve of the recovered fibres did not change, but the tensile strength and elongation at break both decreased by 35%. The recovered fibres still have higher strength and modulus than glass fibres. Therefore, they can still be used in good-quality composite products.

Future study

In a future study, we plant to:

- Investigate advanced separation techniques, such as membrane filtration or extraction methods, to enhance the recovery and reuse of hydrogen peroxide, minimizing distillation costs.
- Investigate the by-products of the process in detail.
- Conduct a detailed economic assessment of the recycling process, considering both the direct costs of hydrogen peroxide reuse and potential savings from reduced waste disposal

Acknowledgements We extend our heartfelt gratitude to the Tshwane University of Technology for supporting and facilitating this research project. Additionally, we express our appreciation to Manufacturing, Engineering, and Related Services SETA (MerSETA) for providing financial assistance, which was instrumental in the successful completion of this study. Special thanks are due to Blackstone Tek for generously supplying us with the necessary raw materials, making this investigation possible and enabling us to obtain valuable insights into carbon fibre recycling. Furthermore, we would like to acknowledge the Council for Scientific and Industrial Research (CSIR) for their invaluable assistance in sample characterization, which significantly contributed to the robustness and reliability of our findings. Their expertise and collaboration were instrumental in ensuring the thorough analysis of the collected data. We acknowledge funding from USDA-NIFA Hatch Project OHO01417. The research reported in this paper was supported by the National Research, Development and Innovation Office (FK138501, FK131882), Hungary. Kolos Molnár was supported by the János Bolyai Scholarship of the Hungarian Academy of Sciences.

Funding Open access funding provided by Budapest University of Technology and Economics.

Declarations

Conflict of interest The authors declare no competing financial interest.

References

1. Vasco JC (2021) Additive manufacturing for the automotive industry. In: Pou J, Riveiro A, Davim JP (eds) Additive manufacturing. Elsevier, Amsterdam, pp 505–530
2. Verma S, Balasubramaniam B, Gupta RK (2018) Recycling, reclamation and re-manufacturing of carbon fibres. Curr Opin Green Sustain Chem 13:86–90. https://doi.org/10.1016/j.cogsc.2018.05.011
3. Yu G-C, Wu L-Z, Feng L-J (2015) Enhancing the thermal conductivity of carbon fibre reinforced polymer composite laminates by coating highly oriented graphite films. Mater Des 88:1063–1070. https://doi.org/10.1016/j.matdes.2015.09.096
4. Zhou F, Zhang J, Song S et al (2019) Effect of temperature on material properties of carbon fibre reinforced polymer (CFRP)

tendons: experiments and model assessment. Materials. https://doi.org/10.3390/ma12071025
5. Moriyama A, Iwahashi H, Fujita K (2024) Assessing cellular responses to milled recycled carbon fibre in alveolar macrophages. J Mater Cycles Waste Manag 26:2128–2137. https://doi.org/10.1007/s10163-024-01950-6
6. Shen M, Huang W, Chen M et al (2020) (Micro)plastic crisis: un-ignorable contribution to global greenhouse gas emissions and climate change. J Clean Prod 254:120138. https://doi.org/10.1016/j.jclepro.2020.120138
7. Sommer V, Walther G (2021) Recycling and recovery infrastructures for glass and carbon fibre reinforced plastic waste from wind energy industry: a European case study. Waste Manag 121:265–275. https://doi.org/10.1016/j.wasman.2020.12.021
8. Zaman AU, Gutub SA, Soliman MF, Wafa MA (2014) Sustainability and human health issues pertinent to fibre reinforced polymer composites usage: a review. J Reinf Plast Compos 33:1069–1084. https://doi.org/10.1177/0731684414521087
9. Danish A, Mosaberpanah MA, Salim MU et al (2022) Utilization of recycled carbon fibre reinforced polymer in cementitious composites: a critical review. J Build Eng 53:104583. https://doi.org/10.1016/j.jobe.2022.104583
10. Zhang J, Chevali VS, Wang H, Wang C-H (2020) Current status of carbon fibre and carbon fibre composites recycling. Compos B Eng 193:108053. https://doi.org/10.1016/j.compositesb.2020.108053
11. Maia BS, Behravesh AH, Tjong J, Sain M (2022) Mechanical performance of modified polypropylene/polyamide matrix reinforced with treated recycled carbon fibres for lightweight applications. J Polym Res. https://doi.org/10.1007/s10965-022-02975-x
12. Rani M, Choudhary P, Krishnan V, Zafar S (2021) A review on recycling and reuse methods for carbon fibre/glass fibre composites waste from wind turbine blades. Compos B Eng 215:108768. https://doi.org/10.1016/j.compositesb.2021.108768
13. Borjan D, Knez Ž, Knez M (2021) Recycling of carbon fibre-reinforced composites—difficulties and future perspectives. Materials 14:4191. https://doi.org/10.3390/ma14154191
14. Abdallah R, Juaidi A, Savaş MA et al (2021) A critical review on recycling composite waste using pyrolysis for sustainable development. Energies. https://doi.org/10.3390/en14185748
15. Czajczyńska D, Krzyżyńska R, Jouhara H, Spencer N (2017) Use of pyrolytic gas from waste tire as a fuel: a review. Energy 134:1121–1131. https://doi.org/10.1016/j.energy.2017.05.042
16. Hao S, He L, Liu J et al (2021) Recovery of carbon fibre from waste prepreg via microwave pyrolysis. Polymers 13:1231. https://doi.org/10.3390/polym13081231
17. Gravgaard DP, Henriksen ML, Hinge M (2024) Dissolution recycling for recovery of polypropylene and glass fibres. J Mater Cycles Waste Manag 26:961–969. https://doi.org/10.1007/s10163-023-01873-8
18. Okajima I, Hiramatsu M, Shimamura Y et al (2014) Chemical recycling of carbon fibre reinforced plastic using supercritical methanol. J Supercrit Fluids 91:68–76. https://doi.org/10.1016/j.supflu.2014.04.011
19. Xu P, Li J, Ding J (2013) Chemical recycling of carbon fibre/epoxy composites in a mixed solution of peroxide hydrogen and N, N-dimethylformamide. Compos Sci Technol 82:54–59. https://doi.org/10.1016/j.compscitech.2013.04.002
20. van de Werken N, Reese MS, Taha MR, Tehrani M (2019) Investigating the effects of fibre surface treatment and alignment on mechanical properties of recycled carbon fibre composites. Compos Part A Appl Sci Manuf 119:38–47. https://doi.org/10.1016/j.compositesa.2019.01.012
21. Schamel E, Wehnert G, Schlachter H, Söthje D (2021) Chemical recycling of carbon fibre reinforced epoxy composites using mild conditions. Chem Ing Tech. https://doi.org/10.1002/cite.202100048
22. Huan X, Shi K, Yan J et al (2020) High performance epoxy composites prepared using recycled short carbon fibre with enhanced dispersibility and interfacial bonding through polydopamine surface-modification. Compos B Eng 193:107987. https://doi.org/10.1016/j.compositesb.2020.107987
23. Keith MJ, Román-Ramírez LA, Leeke G, Ingram A (2019) Recycling a carbon fibre reinforced polymer with a supercritical acetone/water solvent mixture: comprehensive analysis of reaction kinetics. Polym Degrad Stab 161:225–234. https://doi.org/10.1016/j.polymdegradstab.2019.01.015
24. Ray S, Cooney RP (2018) Chapter 9-Thermal degradation of polymer and polymer composites. In: Kutz M (ed) Handbook of environmental degradation of materials, 3rd edn. William Andrew Publishing, Norwich, pp 185–206
25. Shi Z, Zou C, Zhou F, Zhao J (2022) Analysis of the mechanical properties and damage mechanism of carbon fibre/epoxy composites under UV aging. Materials. https://doi.org/10.3390/ma15082919
26. Reitz V, Meinhard D, Ruck S et al (2017) A comparison of IR- and UV-laser pretreatment to increase the bonding strength of adhesively joined aluminum/CFRP components. Compos Part A Appl Sci Manuf 96:18–27. https://doi.org/10.1016/j.compositesa.2017.02.014
27. Azwa ZN, Yousif BF, Manalo AC, Karunasena W (2013) A review on the degradability of polymeric composites based on natural fibres. Mater Des 47:424–442. https://doi.org/10.1016/j.matdes.2012.11.025
28. Wang Y, Li J, Zhou X et al (2020) Chemical degradation of carbon fibre reinforced bismaleimide resin composites to recover carbon fibre and nitrogen doped carbon materials. Compos Sci Technol 199:108342
29. Lee S, Cho SY, Chung YS et al (2022) High electrical and thermal conductivities of a PAN-based carbon fibre via boron-assisted catalytic graphitization. Carbon N Y 199:70–79. https://doi.org/10.1016/j.carbon.2022.07.068
30. Deng J, Xu L, Liu J et al (2020) Efficient method of recycling carbon fibre from the waste of carbon fibre reinforced polymer composites. Polym Degrad Stab. https://doi.org/10.1016/j.polymdegradstab.2020.109419
31. Zhao Q, An L, Li C et al (2022) Environment-friendly recycling of CFRP composites via gentle solvent system at atmospheric pressure. Compos Sci Technol. https://doi.org/10.1016/j.compscitech.2022.109461
32. Major GH, Avval TG, Moeini B et al (2020) Assessment of the frequency and nature of erroneous x-ray photoelectron spectroscopy analyses in the scientific literature. J Vac Sci Technol A 38:061204. https://doi.org/10.1116/6.0000685
33. Weitzsacker CL, Xie M, Drzal LT (1997) Using XPS to investigate fibre/matrix chemical interactions in carbon-fibre-reinforced composites. Surf Interface Anal 25:53–63
34. Qian X, Chen L, Huang J et al (2013) Effect of carbon fibre surface chemistry on the interfacial properties of carbon fibres/epoxy resin composites. J Reinf Plast Compos 32:393–401. https://doi.org/10.1177/0731684412468369
35. Oishi SS, Botelho EC, Rezende MC, Ferreira NG (2017) Structural and surface functionality changes in reticulated vitreous carbon produced from poly(furfuryl alcohol) with sodium hydroxide additions. Appl Surf Sci 394:87–97. https://doi.org/10.1016/j.apsusc.2016.10.112
36. Li H, Wang N, Han X et al (2021) Mechanism identification and kinetics analysis of thermal degradation for carbon fibre/epoxy resin. Polymers. https://doi.org/10.3390/polym13040569
37. Ge L, Li X, Feng H et al (2023) Analysis of the pyrolysis process, kinetics and products of the base components of waste wind

turbine blades (epoxy resin and carbon fibre). J Anal Appl Pyrolysis 170:105919. https://doi.org/10.1016/j.jaap.2023.105919
38. Karuppannan Gopalraj S, Kärki T (2020) A review on the recycling of waste carbon fibre/glass fibre-reinforced composites: fibre recovery, properties and life-cycle analysis. SN Appl Sci 2:433. https://doi.org/10.1007/s42452-020-2195-4
39. Cunliffe AM, Jones N, Williams PT (2003) Recycling of fibre-reinforced polymeric waste by pyrolysis: thermo-gravimetric and bench-scale investigations. J Anal Appl Pyrolysis 70:315–338. https://doi.org/10.1016/S0165-2370(02)00161-4
40. Kooduvalli K, Unser J, Ozcan S, Vaidya UK (2022) Embodied energy in pyrolysis and solvolysis approaches to recycling for carbon fibre-epoxy reinforced composite waste streams. Recycling. https://doi.org/10.3390/recycling7010006
41. Naqvi SR, Prabhakara HM, Bramer EA et al (2018) A critical review on recycling of end-of-life carbon fibre/glass fibre reinforced composites waste using pyrolysis towards a circular economy. Resour Conserv Recycl 136:118–129. https://doi.org/10.1016/j.resconrec.2018.04.013
42. Meng F, Olivetti EA, Zhao Y et al (2018) Comparing life cycle energy and global warming potential of carbon fibre composite recycling technologies and waste management options. ACS Sustain Chem Eng 6:9854–9865. https://doi.org/10.1021/acssuschemeng.8b01026
43. Zhang Y, Li Y, Zhang J et al (2021) High-temperature effect on the tensile mechanical properties of unidirectional carbon fibre-reinforced polymer plates. Materials. https://doi.org/10.3390/ma14237214
44. Shams SS, El-Hajjar RF (2013) Effects of scratch damage on progressive failure of laminated carbon fibre/epoxy composites. Int J Mech Sci 67:70–77. https://doi.org/10.1016/j.ijmecsci.2012.12.008
45. Sukanto H, Raharjo WW, Ariawan D, Triyono J (2021) Carbon fibres recovery from CFRP recycling process and their usage: a review. IOP Conf Ser Mater Sci Eng 1034:012087. https://doi.org/10.1088/1757-899x/1034/1/012087